

Effects of phospholipid unsaturation on the bilayer nonpolar region: a molecular simulation study

Tomasz Róg,* Krzysztof Murzyn,* Ryszard Gurbiel,* Yuji Takaoka,† Akihiro Kusumi,§ and Marta Pasenkiewicz-Gierula^{1,*}

Department of Biophysics,* Faculty of Biotechnology, Jagiellonian University, Kraków, Poland; Department of Molecular Science,† Research Center, Taisho Pharmaceutical Co., Ltd., Omiya, Saitama 330, Japan; and Department of Biological Science,§ Graduate School of Science, Nagoya University, Nagoya, Japan

Abstract Molecular dynamics simulations of two monounsaturated phosphatidylcholine (PC) bilayers made of 1-palmitoyl-2-oleoyl-PC (POPC; *cis*-unsaturated) and 1-palmitoyl-2-elaidoyl-PC (PEPC; *trans*-unsaturated) were carried out to investigate the effect of a double bond in the PC β -chain and its conformation on the bilayer core. Four nanosecond trajectories were used for analyses. A fully saturated 1,2-dimyristoyl-PC (DMPC) bilayer was used as a reference system. In agreement with experimental data, this study shows that properties of the PEPC bilayer are more similar to those of the DMPC than to the POPC bilayer. The differences between POPC and PEPC bilayers may be attributed to the different ranges of angles covered by the torsion angles β_{10} and β_{12} of the single bonds next to the double bond in the oleoyl (O) and elaidoyl (E) chains. Broader distributions of β_{10} and β_{12} in the E chain than in the O chain make the E chain more flexible. In effect, the packing of chains in the PEPC bilayer is similar to that in the DMPC bilayer, whereas that in the POPC bilayer is looser than that in the DMPC bilayer. The effect of the *cis*-double bond on torsions at the beginning of the O chain (β_4 and β_5) is similar to that of cholesterol on these torsions in a myristoyl chain.—Róg, T., K. Murzyn, R. Gurbiel, Y. Takaoka, A. Kusumi, and M. Pasenkiewicz-Gierula. **Effects of phospholipid unsaturation on the bilayer nonpolar region: a molecular simulation study.** *J. Lipid Res.* 2004. 45: 326–336.

Supplementary key words phosphatidylcholine • *cis* double bond • *trans* double bond • skew conformation • chain packing

Phospholipids with two asymmetric hydrocarbon chains, of which one is fully saturated in the γ position and the other is mono-*cis*- or poly-*cis*-unsaturated in the β position, are the most common in nature (1). Among mono-*cis*-unsaturated phosphatidylcholines (PCs), 1-palmitoyl-2-oleoyl-PC (POPC) is the most abundant. In the past, phospholipids with *trans*-unsaturated hydrocarbon chains were believed to be rare in nature. They were found in photo-

synthetic membranes of higher plants (2) and algae (3) as well as in some marine bacteria (4). With advances in separation and quantification techniques, new *trans*-unsaturated lipids have been identified in membranes of prokaryotes (5) and algal chloroplasts (6). In membranes of gram-negative bacteria, the relative proportion of *trans*-unsaturated lipids increases under physiologically stressful conditions, such as increased temperature (7), starvation and desiccation (8), and organic solvents (9). The increase of the *trans*-to-*cis* ratio results from an enzymatically controlled direct *cis*-*trans* isomerization that does not shift the position of the double bond and occurs only at the β position of the glycerol moiety (7). The *cis*-*trans* conversion in the bacterial membrane is believed to be a fast and inexpensive mechanism enabling the membrane to maintain constant fluidity (5).

Experimental (10–13) and molecular modeling (14) studies of model membranes show that in the membrane, a double bond in the *cis* conformation located near the middle of the chain interferes with the hydrocarbon chain packing. This decreases the cooperativity of the chain interactions and causes a substantial decline in the main phase transition temperature (13, 15–18). The effect of a *trans* double bond on the main phase transition temperature of hydrocarbon chains is much weaker (13, 16, 18). A double bond present in a PC chain increases the lateral PC-PC spacing in the bilayer (13). Nevertheless, the order and reorientational motion of saturated and *cis*-unsaturated (19, 20) as well as *trans*-unsaturated (21) hydrocarbon chains in model membranes are similar. In contrast, the translational diffusion of lipids (21–23) as well as small lipid-soluble molecules (24, 25) is significantly lower in *cis*- and *trans*-unsatu-

Abbreviations: DMPC, 1,2-dimyristoyl-phosphatidylcholine; E, elaidoyl; M, myristoyl; MD, molecular dynamics; O, oleoyl; PC, phosphatidylcholine; PEPC, 1-palmitoyl-2-elaidoyl-phosphatidylcholine; POPC, 1-palmitoyl-2-oleoyl-phosphatidylcholine; PSPC, 1-palmitoyl-2-stearoyl-phosphatidylcholine; RAF, reorientational autocorrelation function; RDF, radial distribution function; SA, surface area.

¹ To whom correspondence should be addressed.
e-mail: mpga@mol.uj.edu.pl

Manuscript received 5 May 2003 and in revised form 24 October 2003.

Published, JLR Papers in Press, November 1, 2003.

DOI 10.1194/jlr.M300187-JLR200

rated bilayers than in saturated bilayers. The introduction of a double bond into the alkyl chain decreases water penetration of the bilayer; the effect is greater for *cis*-unsaturated than for *trans*-unsaturated bilayers (26).

Among several reports on computer simulations of unsaturated PC bilayers (27–38), *cis*- and *trans*-unsaturated bilayers were compared in two of them (27, 36). In a Langevin dynamics simulation study, Pearce and Harvey (27) showed that structural and dynamic properties of PCs with a *trans* double bond are similar to those of saturated PCs, whereas PCs with a *cis* double bond behave differently. In a comparative molecular dynamics (MD) simulation study, Murzyn et al. (36) showed that numbers of inter-lipid interactions via water bridges and charge pairs in *cis*- and *trans*-unsaturated PC bilayers are similar and that both are smaller than in a saturated 1,2-dimyristoyl-PC (DMPC) bilayer.

Scarce experimental (10, 39) and molecular modeling (40–42) studies of mixed-chain phospholipids indicate that in mono-*cis*-unsaturated chains, torsion angles of the single bonds next to the double bond are highly distributed around *skew* (120°), *skew'* (240°), and *trans* (180°) conformations. The estimated distribution of angles ranges from 90 to 175° and -90 to -175° for the *skew* and *skew'* conformations (10). This follows from the steric energy profile (41), which has two broad minima centered at $\pm 110^\circ$, a relatively narrow and low-energy barrier centered at 180° , and a broad, higher energy barrier extending from -60° (*gauche*⁻) to 60° (*gauche*⁺) with a small maximum at 0° . Thus, torsion angles of the single bonds next to the double bond are unlikely to have conformations from the range \langle *gauche*⁻ to *gauche*⁺ \rangle . Similar results were obtained from quantum mechanical calculations of two model compounds, each containing two *cis*-unsaturated bonds, as well as from MD simulations of the poly-*cis*-unsaturated docosahexaenoic chain (32). Molecular modeling calculations indicate that the *gauche* probability of the torsion angles second next to the *cis* double bond is higher than that in fully saturated chains (39, 40). Both experimental (43) and molecular modeling (40) studies indicate that a single *cis* double bond in the phospholipid β -chain has practically no effect on the fully saturated γ -chain. To our knowledge, the effects of the *trans* double bond in the β -chain on the neighboring torsion angles or the γ -chain have not been determined either experimentally or from simulations.

The aim of the present MD simulation study was to determine the effect of PC monounsaturations and the conformation (*cis* or *trans*) of the double bond in the β -chain on hydrocarbon chain order, packing, and dynamics in the membrane. Two PC bilayers were studied: POPC (mono-*cis*-unsaturated) and 1-palmitoyl-2-elaidoyl-PC (PEPC; mono-*trans*-unsaturated) together with a third, DMPC (fully saturated), used as a reference system. It is true that a bilayer made of fully saturated 1-palmitoyl-2-stearoyl-PC (PSPC) would constitute a better reference system for the POPC and PEPC bilayers (the length of corresponding alkyl chains of the three lipids is the same), but there is a serious problem in doing this. Unfortunately, there are very few experimental data for a PSPC bilayer, and this makes the generation of a computer model for this bilayer uncertain and

unreliable and therefore unsuitable as a comparison. By contrast, reliable data for the DMPC bilayer are available, making this a safe reference system for comparative studies. The much lower temperature of the main phase transition of DMPC compared with PSPC is an additional advantage for this choice, because the three bilayers are all now in the liquid crystalline phase at the physiological temperature of 37°C . DMPC and POPC bilayers were simulated for 15 ns and the PEPC bilayer for 8 ns. Analyses of the trajectories generated in the MD simulations confirmed that the *cis* double bond (torsion β_{11}) promotes the conformational variability of the neighboring torsion angles (β_{10} and β_{12}), consistent with both the experimental and MD simulation data. In addition, they showed that the *trans* double bond has a similar effect, although the range of angles that β_{10} and β_{12} assume is broader. Indeed, β_{10} and β_{12} of the oleoyl (O; *cis*) chain cover angles between 60 and 300° , whereas those of the elaidoyl (E; *trans*) chain cover the whole range of angles, i.e., between 0 and 360° .

METHODS

Simulation systems

POPC, PEPC, and DMPC bilayers used in this study consisted of 72 ($6 \times 6 \times 2$) PC molecules. POPC and PEPC bilayers were hydrated with 1,922 water molecules; the DMPC bilayer was hydrated with 1,622 water molecules (in each bilayer, water constituted $\sim 39\%$ by weight). The structure, numbering of atoms, and torsion angles in POPC, PEPC, and DMPC molecules are shown in Fig. 1.

The β -chain of POPC and PEPC has one double bond between C9 and C10 (Fig. 1). In POPC, the double bond is in the *cis* conformation (O chain), and in PEPC, it is in the *trans* conformation (E chain), so the torsion angle for the double bond, β_{11} , is 0° for POPC and 180° for PEPC. The β - and γ -chains of DMPC [myristoyl (M) chain] and the γ -chain of POPC and PEPC are fully saturated. Details concerning the construction of the POPC and PEPC molecules and subsequently bilayers, as well as the initial simulations of these bilayers, were described in Murzyn et al. (36). Details concerning the DMPC bilayer were described in Pasenkiewicz-Gierula et al. (44, 45).

Simulation parameters

For PCs, optimized potentials for liquid simulations (OPLS) parameters (46), and for water, TIP3P parameters (47), were used. The united-atom approximation was applied to the CH, CH₂, and CH₃ groups of PCs. The atomic charges on head groups of DMPC, POPC, and PEPC were practically the same; details are given in Pasenkiewicz-Gierula et al. (45). Procedures for supplementing the original OPLS base with the missing parameters for the PC head group were described in Pasenkiewicz-Gierula et al. (45), and those for the β -chain sp² carbon atoms were described in Murzyn et al. (36).

Simulation conditions

POPC and PEPC bilayers were simulated for 15 and 8 ns, respectively, initially using the MD AMBER 4.0 (48) and then (last 5 ns) AMBER 5.0 (49) packages. Three-dimensional periodic boundary conditions with the usual minimum image convention were used. The SHAKE algorithm (50) was used to preserve the bond lengths of the water molecule, and the time step was set at 2 fs (51). Restraints of a flat-bottom harmonic potential as de-

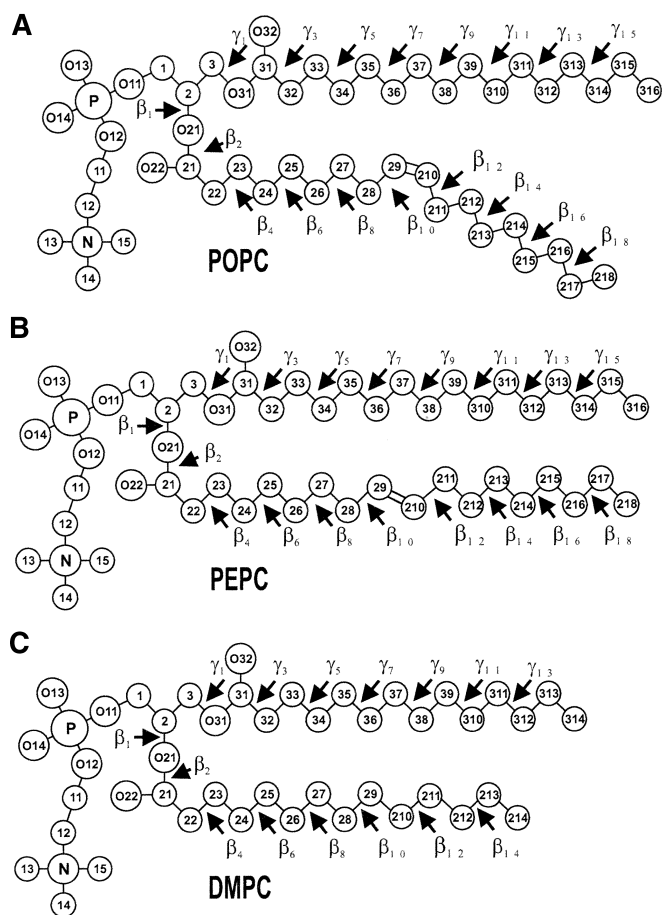


Fig. 1. Molecular structures with numbering of atoms and torsion angles of 1-palmitoyl-2-oleoyl-phosphatidylcholine (POPC) (A), 1-palmitoyl-2-elaidoyl-phosphatidylcholine (PEPC) (B), and 1,2-dimyristoyl-phosphatidylcholine (DMPC) (C). The chemical symbol for carbon atoms (C) is omitted.

finer and implemented in the AMBER package (49) were imposed on the double bond to prevent *cis-trans* isomerization. As neither the POPC nor the PEPC bilayer contains charge molecules, a residue-based cutoff with a cutoff distance of 12 Å was used to calculate the nonbonded interactions. The list of nonbonded pairs was updated every 25 steps. Other computational details are given in Murzyn et al. (36).

The MD simulations were carried out at a constant pressure (1 atm) and at a temperature of 310 K (37°C), which is above the main phase transition temperature for the POPC (−5°C) (18), PEPC (26°C) (18), and DMPC (23°C) bilayers. The temperatures of the solute and solvent were controlled independently. Both the temperature and pressure of the systems were controlled by the Berendsen method (52). The relaxation times for temperatures and pressure were set at 0.4 and 0.6 ps, respectively. The applied pressure was controlled anisotropically, each direction being treated independently with the trace of the pressure tensor kept constant for 1 atm. The DMPC bilayer was simulated for 15 ns under similar MD simulation conditions (44, 45).

RESULTS

Details concerning the equilibration and validation of POPC and PEPC bilayers were described in Murzyn et al.

(36), and those concerning the DMPC bilayer were described in Pasenkiewicz-Gierula et al. (45). For the analyses described below, the last 4 ns fragments of the generated trajectories were used. Errors in the derived average values are standard error estimates obtained from the block-averaging procedure. Because the torsion angles β_3 and γ_3 (Fig. 1) are not in well defined, stable conformations (*trans* or *gauche*) (53), when calculating conformation-related quantities, β_3 and γ_3 as well as the third segmental vector were not considered.

Cross-sectional area per PC

The average surface area (SA) per PC is $64.3 \pm 0.6 \text{ \AA}^2$ in POPC, $63.5 \pm 0.6 \text{ \AA}^2$ in PEPC, and $60.2 \pm 0.6 \text{ \AA}^2$ in DMPC bilayers. The values for the POPC and DMPC bilayers are in good agreement with those published in the literature. SA/PC in the POPC bilayer was estimated to be 63 \AA^2 from POPC monolayer studies at the surface pressure of 30 mN/m (54) and 66 \AA^2 at the surface pressure of 20 mN/m (55). For the DMPC bilayer, the best estimate for SA/PC is $\sim 60 \text{ \AA}^2$ (56). For the PEPC bilayer, there are no published experimental data.

Molecular order parameter of PC alkyl chains

The molecular order parameter, S_{mol} , profiles [for definition, see Róg and Pasenkiewicz-Gierula (53)] along the β - and γ -chains in the POPC, PEPC, and DMPC bilayers are shown in Fig. 2. Shapes of the profiles for the O and E chains agree well with those given in Seelig and Waespe-Sarčević (18). For the POPC γ -chain, the S_{mol} profile agrees with that of Holte et al. (43) and Seelig and Waespe-Sarčević (18). As can be seen from Fig. 2, S_{mol} profiles for β -chains as well as γ -chains of POPC, PEPC, and DMPC are similar, except for segments 10 and 11 of the O chain (i.e., segments that include the *cis* double bond), for which S_{mol} values are substantially lower. Average S_{mol} values for the POPC and PEPC chains are only slightly lower than those for the DMPC chains (Table 1), so saturated, mono-*cis*-unsaturated, and mono-*trans*-unsaturated chains are similarly ordered.

Tilt of PC alkyl chains

The tilt angle of a PC chain as well as the Δ segment (C-C bonds 4–9 above the double bond) and the ω segment (C-C bonds 10–17 below the double bond) of the O and E chains were derived as shown in

$$\arccos\left(\sqrt{\langle \cos^2 \theta \rangle}\right) \quad (\text{Eq. 1})$$

where θ is the angle between the bilayer normal and the average segmental vector (averaged over appropriate segmental vectors ≥ 4) (the n th segmental vector links $n - 1$ and $n + 1$ carbon atoms in the alkyl chain), and $\langle \rangle$ denotes both the ensemble and the time average. The distributions of tilt angles of β - and γ -chains in the POPC, PEPC, and DMPC bilayers are shown in Fig. 3A, B and those of the Δ and ω segments are shown in Fig. 3C, D. Average tilts of the PC chains, given in Table 1, are similar in the three bilayers. Also, tilts of the Δ and ω segments are

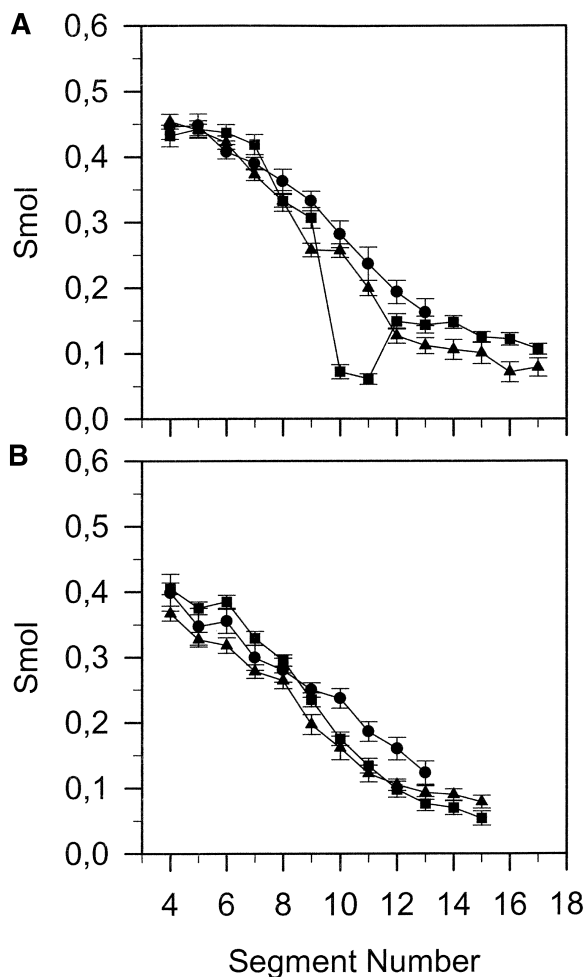


Fig. 2. Profiles of the molecular order parameter (S_{mol}) along the β -chain (A) and γ -chain (B) in the POPC (closed squares), PEPC (closed triangles), and DMPC (closed circles) bilayers. The error bars indicate SEM. Average values of S_{mol} are given in Table 1.

similar in the POPC and PEPC bilayers, but in both bilayers, the Δ segment is significantly less tilted than the ω segment (Table 1). A large difference between the O and E chains is seen in distributions (Fig. 4) and average values

TABLE 1. Average values of parameters

PC	$S_{mol} \pm 0.01$		Tilt ± 1.0					$gauche \pm 0.05$		Lifetime <i>trans</i> / <i>gauche</i> $\pm 4/2$	
	β	γ	β	Δ	ω	II	γ	β	γ	β^a	γ
			°					n		ps	
POPC	0.24	0.22	25	26	41	49	28	3.2	3.0	180/65	180/60
PEPC	0.24	0.20	26	26	39	38	29	3.1	3.0	180/65	180/60
DMPC	0.33	0.26	27	—	—	39 ^b	28	2.5	2.4	180/55	180/55

The molecular order parameter (S_{mol}); tilt angles of the β - and γ -chains, the Δ - and ω -segments, and the double bond (II); numbers of *gauche* rotamers per phosphatidylcholine (PC) chain; and lifetimes of *trans* and *gauche* conformations in 1-palmitoyl-2-oleoyl-PC (POPC), 1-palmitoyl-2-elaidoyl-PC (PEPC), and 1,2-dimyristoyl-PC (DMPC) bilayers. The errors in the average values are SEM estimates.

^a Torsion angles β_{10} and β_{12} are not included.

^b Average tilt of the single C29-C210 bond of the DMPC β -chain (cf. Fig. 1).

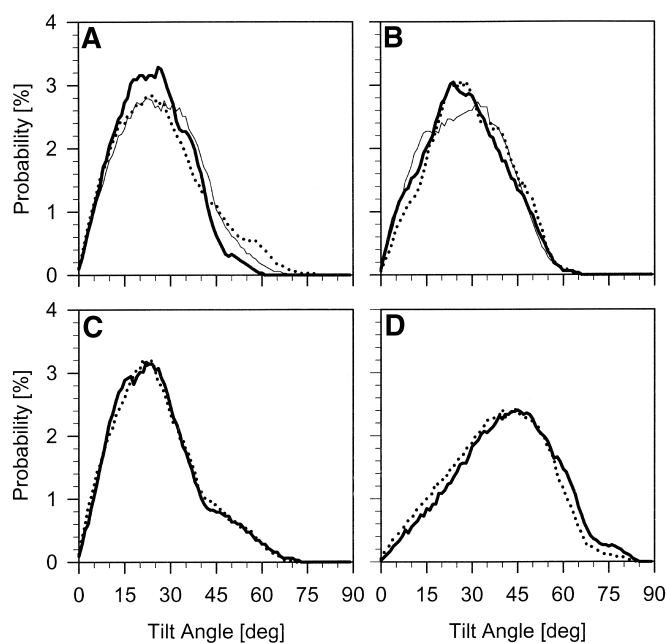


Fig. 3. Distribution of tilt angles of the β -chain (A) and γ -chain (B) of POPC (thick line), PEPC (dotted line), and DMPC (thin line) as well as the Δ -segment (C) and ω -segment (D) of the β -chain of POPC (thick line) and PEPC (dotted line). Average tilt angles are given in Table 1.

(Table 1) of tilt angles of the double bonds. The average tilt of the *cis* double bond is 11° larger than that of the *trans* double bond, which, on the other hand, is similar to that of the single C9-C10 bond in the M chain.

Conformation of PC alkyl chains

Probability profiles of the *gauche* conformation for C-C bonds along the β - and γ -chains in the POPC, PEPC, and DMPC bilayers are shown in Fig. 5A, B (the *gauche* probability for the double bond is zero). The *cis* double bond has a strong effect on the torsion angles of single bonds at the beginning (β_4 and β_5) and middle (β_9 , β_{10} , β_{12} , and β_{13}) of the β -chain. β_4 and β_5 have significantly higher and lower *gauche* probabilities, respectively, than their counterparts in the fully saturated M chain. A similar ef-

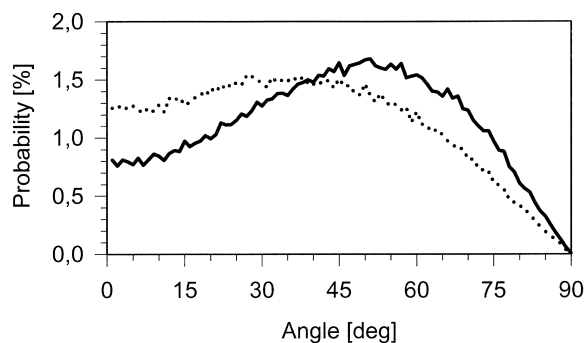


Fig. 4. Distribution of tilt angles of the double bond in the β -chain of POPC (thick line) and PEPC (dotted line).

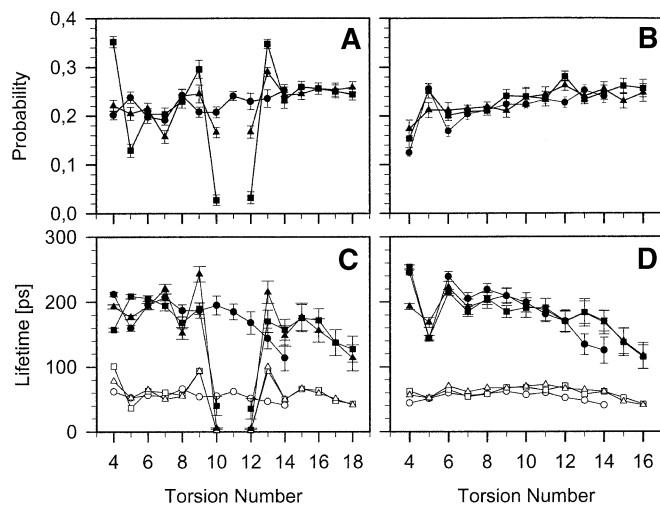


Fig. 5. Probability profiles of the *gauche* conformation along the β -chain (A) and γ -chain (B) in the POPC (closed squares), PEPC (closed triangles), and DMPC (closed circles) bilayers. Lifetimes of the *gauche* conformation (open symbols) and *trans* conformation (closed symbols) along the β -chain (C) and γ -chain (D) in the POPC (squares), PEPC (triangles), and DMPC (circles) bilayers.

fect was brought about in the DMPC β -chain by cholesterol (53). The *gauche* probability of β_{10} and β_{12} (next to the double bond) is zero, and that of β_9 and β_{13} (second next to the double bond) is higher than that in the M chain. The *trans* double bond does not influence torsion angles at the beginning of the β -chain but, like the *cis* double bond, increases the *gauche* probability of β_9 and β_{13} , although to a lesser extent. The *gauche* probability for β_{10} and β_{12} in the E chain is nonzero but is distinctly lower than that in the M chain. The double bond (*cis* or *trans*) has practically no effect on the *gauche* probability along the γ -chain.

Populations of conformations of torsion angles that are first (β_{10} and β_{12}) and second (β_9 and β_{13}) neighbors of the double bond in the POPC and PEPC bilayers are illustrated in **Fig. 6**. β_9 and β_{13} of both the O and E chains assume discrete low-energy conformations (*trans* or *gauche*) in 99% of cases (Fig. 6A, B, G, H), whereas β_{10} and β_{12} of both the O and E chains continuously populate angles between 60 and 300° and 0 and 360°, respectively, with an apparent single maximum at 180° (Fig. 6C–F). Detailed inspection reveals that the distributions of conformations of β_{10} and β_{12} in the O chain have shoulders indicating nonuniform populations of the angles. Indeed, time profiles of the β_{12} conformation in some cases have a bimodal character (**Fig. 7A**).

Correlations between values of torsion angles for pairs of angles neighboring the *trans* double bond in the PEPC bilayer are shown as contour plots in **Fig. 8**. For comparison, a contour plot for a pair of “typical” torsion angles (γ_7 and γ_8) in the γ -chain is also shown (Fig. 8A). For the γ_7 - γ_8 pair, five regions on the plot can be recognized, one for *trans-trans* conformations and four for *trans-gauche* conformations (Fig. 8A). *Gauche-gauche* conformations are much less populated, so they do not appear on the plot.

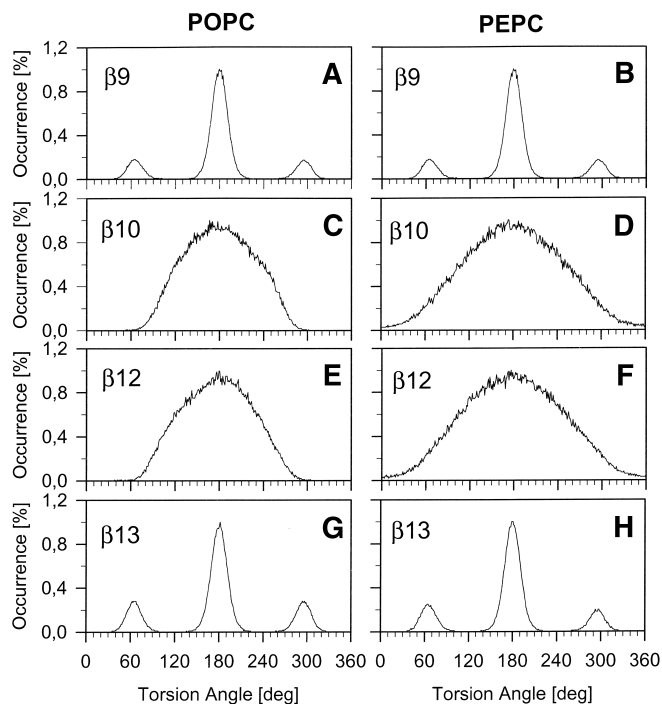


Fig. 6. Populations of the torsion angles β_9 (A, B), β_{10} (C, D), β_{12} (E, F), and β_{13} (G, H) in the POPC (A, C, E, G) and PEPC (B, D, F, H) bilayers. Angles around 60, 180, and 300° correspond to *gauche*⁺, *trans*, and *gauche*⁻ conformations, respectively.

Torsion angles β_{10} and β_{12} do not reside in the low-energy conformations typical for single C-C bonds; therefore, they cover different regions on the plot. For discrete *trans*, *gauche*⁺, and *gauche*⁻ conformations of β_9 and β_{13} , the values of β_{10} and β_{12} cover nearly the whole range of angles (Fig. 8B, C) (relatively less populated conformations do not appear on the plot). The contour plot for the β_{12} - β_{10} pair shows that conformations of these torsion angles are uncorrelated (Fig. 8D); the region covered on the plot is a simple superposition of these angle distributions (cf. Fig. 6D, F). Similar results were obtained for torsion angles next to the *cis* double bond (data not shown).

Conformation lifetimes

Figure 6C, D shows that β_{10} and β_{12} of the O and E chains have a nonzero probability to populate any angle in the range between 60 and 300° and 0 and 360°, respectively. This means that these torsion angles do not have stable conformations. Figure 7A, B well illustrates the instability of the conformational states of β_{12} in the O and E chains. Other single C-C bonds in PC hydrocarbon chains assume low-energy *trans* and *gauche* conformations, as illustrated in Fig. 7C. Lifetime profiles of these conformations along the β - and γ -chains in the POPC, PEPC, and DMPC bilayers are shown in Fig. 5C, D. Lifetimes of *gauche* conformations for POPC β_{10} and β_{12} were set to zero because these angles are never *gauche*. Lifetimes of *trans* conformations for POPC β_{10} and β_{12} as well as *trans* and *gauche* conformations for PEPC β_{10} and β_{12} are very

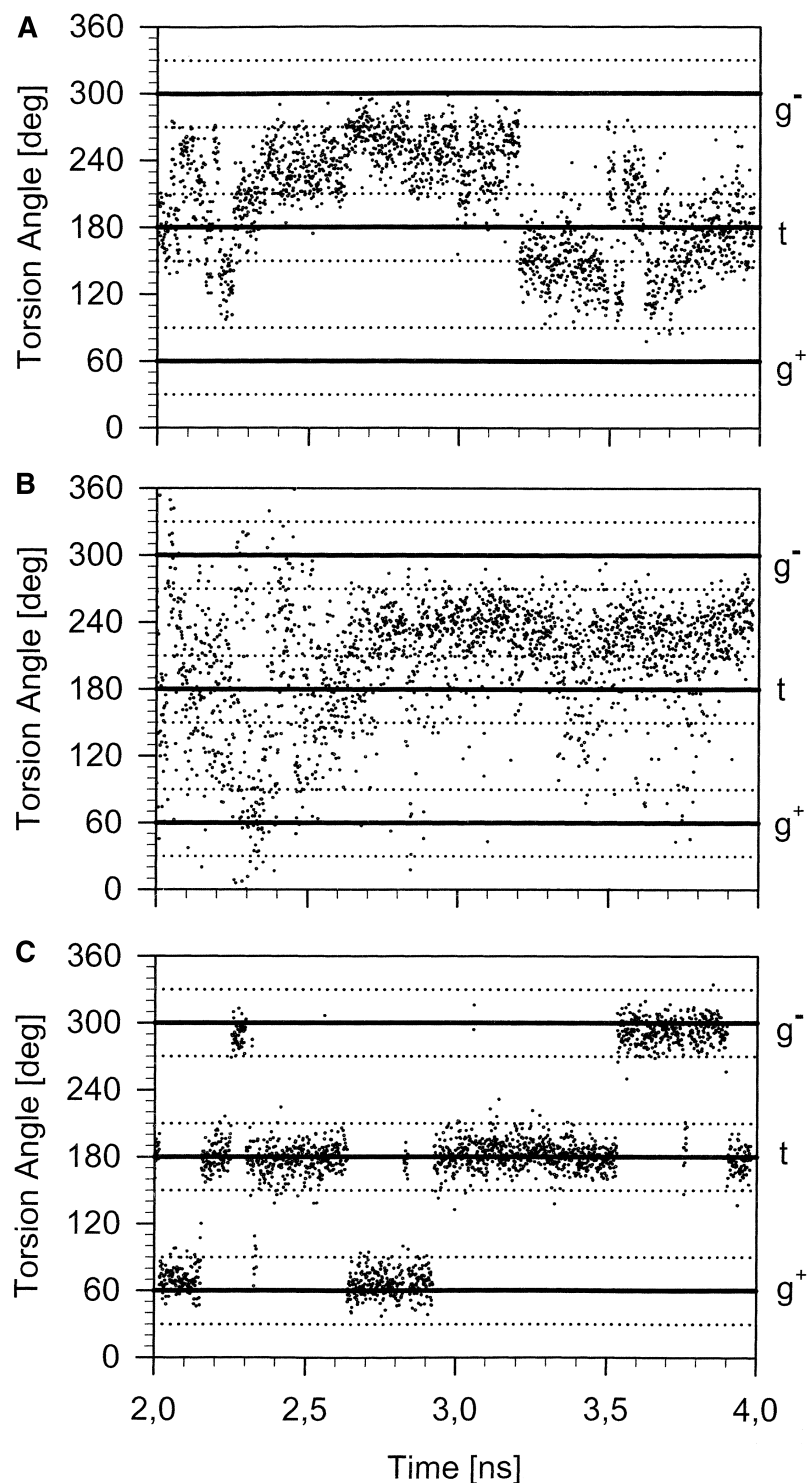


Fig. 7. Time profiles of conformations of the torsion angles β_{12} of arbitrarily chosen POPC (A) and PEPC (B) molecules and γ_{12} of an arbitrarily chosen PEPC molecule (C). *Trans*, *gauche*⁺, and *gauche*⁻ are indicated at right as t, g⁺, and g⁻, respectively. The dashed lines indicate the ranges of angles that characterize a given conformation.

short, which indicates that these conformations are very unstable. For β_9 and β_{13} of the O and E chains, lifetimes of the *gauche* conformation increase by the same amount relative to those of the M chain, whereas lifetimes of the *trans* conformation increase for β_9 and β_{13} of only the E

chain. This is the likely reason why the probability of *gauche* for β_9 and β_{13} of the O chain is higher than that of the E chain (Fig. 5A). For torsion angles other than β_9 , β_{10} , β_{12} , and β_{13} , lifetimes of both the *trans* and *gauche* conformations are similar in all three bilayers.

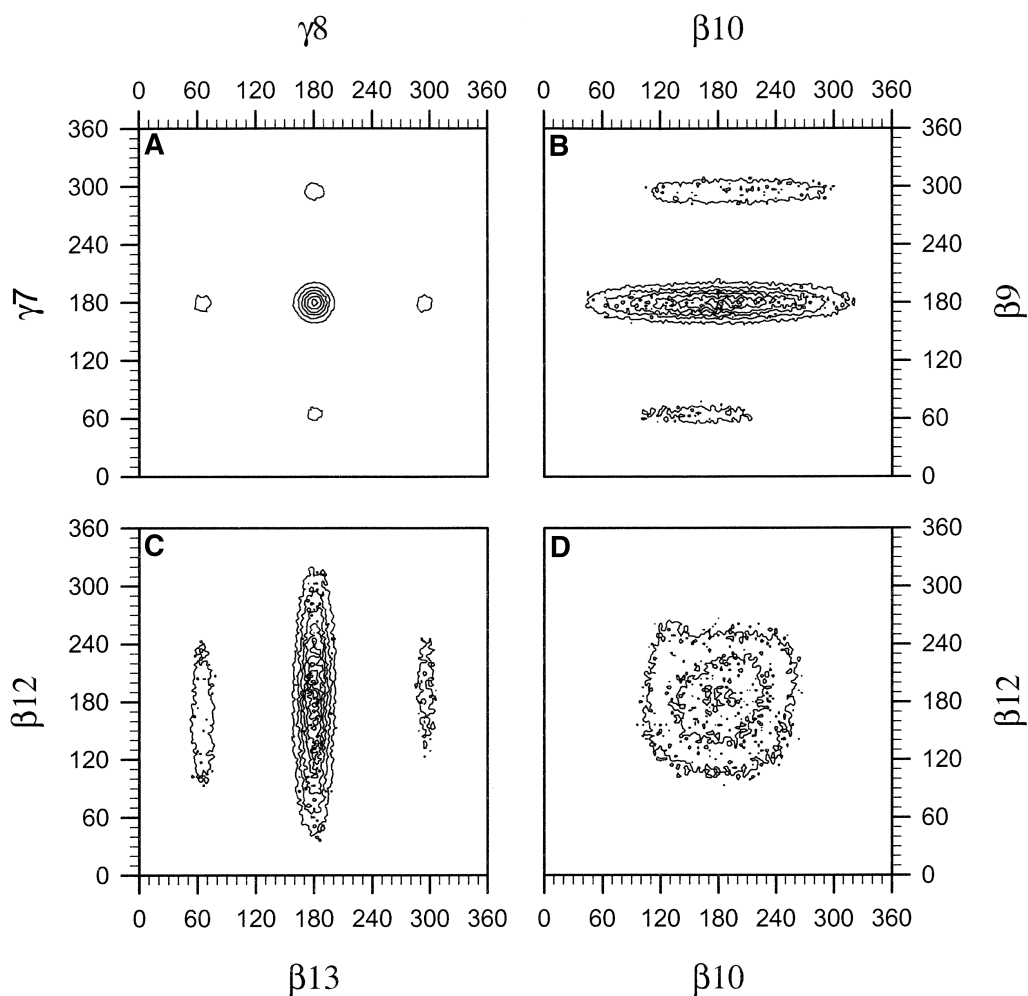


Fig. 8. Contour plots showing correlations between values of torsion angles for the pairs of angles $\gamma 7$ and $\gamma 8$ (A), $\beta 9$ and $\beta 10$ (B), $\beta 12$ and $\beta 13$ (C), and $\beta 10$ and $\beta 12$ (D) in the PEPC bilayer. In A, contours are plotted at intervals of 10, and in B–D, they are plotted at intervals of 2.

Chain packing in the hydrophobic core

Radial distribution functions (RDFs) calculated for the center of mass of the PC alkyl chains belonging to different PC molecules in the POPC, PEPC, and DMPC bilayers are shown in **Fig. 9A**. A broad first maximum and the lack of a second maximum in the RDF for the POPC bilayer indicate that the *cis* double bond disrupts a regular chain packing observed in the DMPC and PEPC bilayers (Fig. 9A).

The RDFs were decomposed into RDFs for the β -chains (a β - β RDF; Fig. 9B), β - and γ -chains (a β - γ RDF; Fig. 9C), and γ -chains (a γ - γ RDF; Fig. 9D). As indicated in Fig. 9B, saturated β -chains pack much better than unsaturated β -chains, but *trans*-unsaturated chains pack better than *cis*-unsaturated chains. The γ - γ RDFs in Fig. 9D show that the γ -chains in the DMPC and PEPC bilayers are arranged regularly, whereas the γ -chains in the POPC bilayer are not. In contrast, as the β - γ RDFs in Fig. 9D show, the arrangement of the unsaturated β -chains relative to γ -chains in both the POPC and PEPC bilayers is more regular than that of the saturated β -chains relative to γ -chains in the DMPC bilayer. One can conclude that in the vicinity of a

cis-unsaturated β -chain in the POPC bilayer, there are mainly saturated γ -chains, whereas in the DMPC bilayer, a β -chain is surrounded by β -chains and a γ -chain is surrounded by γ -chains.

Rotational diffusion

Reorientational autocorrelation functions (RAFTs) were calculated for the Legendre polynomial P1 for β -chain and γ -chain vectors (**Fig. 10A, B**) in the POPC, PEPC, and DMPC bilayers. The β -chain (γ -chain) vector is a vector linking the middle of the C21-C22 (C31-C32) bond (Fig. 1) and the center of gravity of the chain. The RAFT curves could not be satisfactorily fitted to a sum of exponentials; thus, the results presented are only qualitative. The effect of the double bond on the alkyl chain rotation is weak, independent of the bond conformation. A similar conclusion was drawn from spin-label studies of bilayers made of saturated, *cis*-unsaturated, and *trans*-unsaturated PCs (21). In those studies, however, the effects of unsaturation on the chain reorientational motion were monitored indirectly via the reporter group of the spin-label molecule.

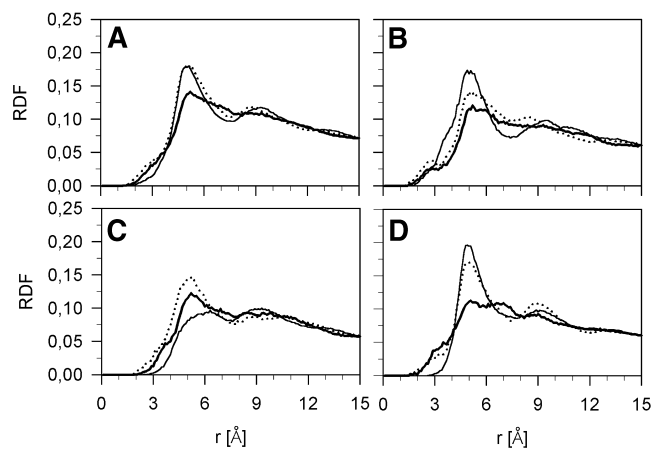


Fig. 9. Radial distribution functions (RDFs) calculated for the centers of masses of the phosphatidylcholine (PC) alkyl chains belonging to different PC molecules for all chains (A), the β -chains relative to a β -chain (B), the β -chains relative to a γ -chain (C), and the γ -chains relative to a γ -chain (D) in the POPC (thick line), PEPC (dotted line), and DMPC (thin line) bilayers.

DISCUSSION

In our previous paper (36), no significant effect of the conformation (*cis* or *trans*) of the double bond in the PC β -chain was found on the organization of the bilayer-water interface. In this paper, details of the effect of the double bond and its conformation on the organization of the bilayer core were investigated. In the MD simulation study, properties of the hydrocarbon core of the mono-*cis*-unsaturated (POPC), mono-*trans*-unsaturated (PEPC), and fully saturated (DMPC) bilayers were compared.

Average parameters characterizing monounsaturated PC bilayers in the liquid crystalline state obtained in this study are similar to those derived experimentally, in spite of the limited size of the computer models. In particular, the mean SA per PC in the POPC (and PEPC) bilayer of $\sim 64 \text{ \AA}^2$ agrees with experimental estimates (54, 55) and, as the experiments predict (13), is greater than that in the DMPC bilayer of $\sim 60 \text{ \AA}^2$. Profiles of the order parameter for the O and E chains have shapes similar to those obtained from NMR spectroscopy (18). In accord with the experimental data of Subczynski and Wisniewska (21), saturated, mono-*cis*-unsaturated, and mono-*trans*-unsaturated chains are similarly ordered, and as Holte et al. (43) showed, mono-*cis*-unsaturation in the β -chain has a minor effect on the order of the γ -chain.

The effect of the *cis* double bond on the β_4 and β_5 torsions angles in the pure POPC bilayer is similar to that of cholesterol in the DMPC-cholesterol bilayer (53). In both bilayers, the *gauche* probability of the β_4 is significantly higher and that of the β_5 is significantly lower than the respective probabilities for the DMPC β -chain in the pure DMPC bilayer. This is a very interesting but puzzling result, because in the first case, the effect is caused by an intrinsic molecular factor, whereas in the second case, it is driven by intermolecular interaction. The changes in the *gauche* probability of β_4 and β_5 are most likely attributable

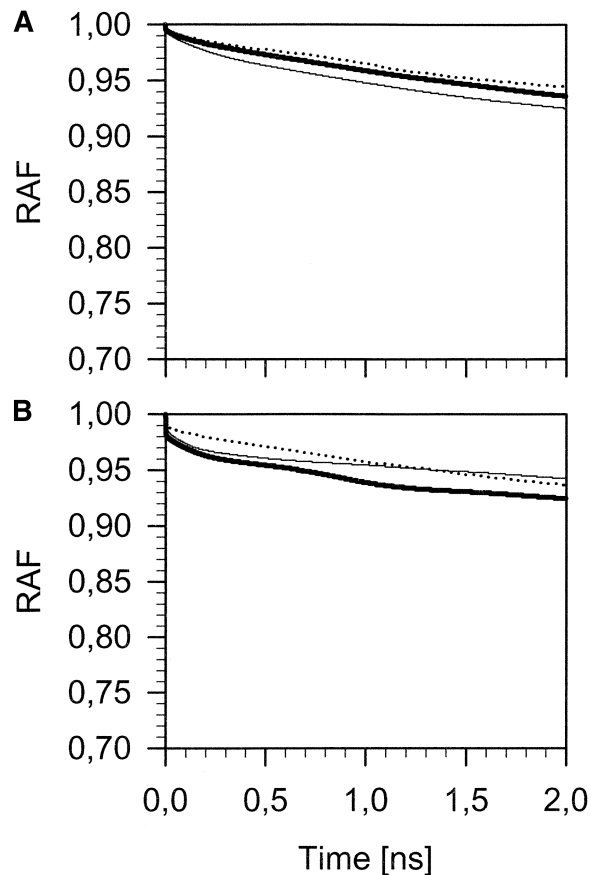


Fig. 10. Reorientational autocorrelation functions (RAFTs) for the β -chain vector (A) and the γ -chain vector (B) in the POPC (thick line), PEPC (dotted line), and DMPC (thin line) bilayers.

to steric effects, but in the framework of the present study, their origin cannot be clearly indicated. Similar effects of the *cis* double bond and cholesterol may explain why water penetration through the POPC and DMPC-cholesterol bilayers is decreased similarly compared with that in the pure DMPC bilayer (26). The *trans* double bond has no effect on the β_4 and β_5 torsions angles.

Detailed conformational analyses of mono- and poly-*cis*-unsaturated chains indicate that torsion angles of saturated C-C bonds next to the double bond have broad distributions around the *skew*, *skew'*, and *trans* conformations, with a low probability of conformations between *gauche*⁻ and *gauche*⁺ (10, 32, 41). On the other hand, molecular mechanics calculations indicated that the *gauche* probability for the second next torsions to the double bond is higher than that in a fully saturated chain (39–41). To our knowledge, the effect of the mono-*trans*-unsaturated bond on the conformation of the neighboring single bonds has not been described in the literature.

Our MD simulation study demonstrated that both *cis* and *trans* double bonds strongly modify conformational states of the next (β_{10} and β_{12}) and second next (β_9 and β_{13}) torsion angles. The distributions of β_{10} and β_{12} are continuous and broad, with maxima at 180° (Fig. 6). The range of angles covered by β_{10} and β_{12} depends on the conformation of the double bond. The values of β_{10} and

β_{12} in the O chain are between 60 and 300° (Fig. 6C, E), whereas in the E chain, they cover the whole range of angles between 0 and 360° (Fig. 6D, F). The result for the O chain is in accord with results from single crystal studies by Keneko, Yano, and Sato (10) and molecular mechanics calculations by Li et al. (41). The result for the E chain is an evidently new result of the present study; unfortunately, no experimental data are available to verify it.

Different ranges of angles covered by β_{10} and β_{12} in the O and E chains are the most likely explanation for the experimentally observed differences in the properties of the POPC and PEPC bilayers. A wider distribution of β_{10} and β_{12} in the E chain makes the chain more flexible. Moreover, the distribution of *gauche* rotamers along the E chain and the inclination of the C9=C10 bond are more similar to those of the M than of the O chain (Fig. 5A). Thus, the E chain is more adaptive than the O chain and, in many respects, displays properties similar to those of the M chain. This result is in agreement with the reported similarity in the subcell structure and the occurrence of polytypic structures of mono-*trans*-unsaturated and fully saturated fatty acid crystals (57). Also, it is in agreement with the conclusion drawn from experimental observation that cholesterol mixes well with saturated and mono-*trans*-unsaturated phospholipids but not with mono-*cis*-unsaturated phospholipids (24, 58).

A greater similarity of the E chain to the M than to the O chain is also reflected in chain-chain RDFs (Fig. 9). The RDFs indicate that both mono-*trans*-unsaturated and fully saturated chains pack more regularly in the bilayer than the less adaptive mono-*cis*-unsaturated chains (Fig. 9A). Thus, the generally higher main phase transition temperatures of saturated and mono-*trans*-unsaturated bilayers than mono-*cis*-unsaturated bilayers may be attributed mainly to the observed differences in the chain packing. The RDFs shown in Fig. 9B, D indicate that, in contrast to the DMPC and PEPC bilayers, the β -chains as well as the γ -chains in the POPC bilayer are not arranged regularly relative to each other. Nevertheless, spatial ordering of β -chains relative to γ -chains is more apparent in the POPC and PEPC bilayers than in the DMPC bilayer (Fig. 9C).

Our MD simulation study confirmed an earlier Langevin dynamics simulation study of Pearce and Harvey (27) that showed that structural and dynamic properties of PCs with a *trans* double bond are similar to those of saturated PCs. Most likely, as a result of this similarity, phospholipids with *trans*-unsaturated hydrocarbon chains are much less abundant in nature than those with *cis*-unsaturated hydrocarbon chains.

In membranes of some bacteria, the relative proportion of *trans*-unsaturated fatty acids increases under physiologically stressful conditions (7–9). The increase results from an enzymatically controlled direct *cis-trans* isomerization of the double bond (7). *Cis-trans* isomerization was proposed as a biological mechanism of the regulation of bacterial membrane fluidity (5). The *cis* bond would increase fluidity, whereas the *trans* bond would decrease it. Unfortunately, experimental results (21–23) and the MD simulation results presented here do not support this hypothesis.

They indicate that the lateral self-diffusion of *cis*-unsaturated lipids in the bilayer is slower than that of *trans*-unsaturated lipids, whereas the rotational diffusion is similar. Furthermore, S_{mol} profiles for *cis*- and *trans*-unsaturated chains have similar overall shapes. Thus, at temperatures above the main phase transition temperature for *trans*-unsaturated chains, the double bond in either the *cis* or the *trans* conformation has little effect on membrane fluidity and order. However, the biological role of *cis-trans* isomerization of the double bond in bacterial fatty acids might stem from differences in the interactions of other membrane components with *cis*- and *trans*-unsaturated chains. It has been demonstrated that membranes of bacteria living in extreme conditions contain polar carotenoids (59, 60). Carotenoids and cholesterol have similar effects on alkyl chains of phospholipids (61, 62) and both affect *cis*-unsaturated chains less strongly than saturated chains (26, 61, 62); in the case of cholesterol, the effect is also less strong than that of *trans*-unsaturated chains (26). Because of the similarity of saturated and *trans*-unsaturated chains discussed above, one can expect that the effect of carotenoids on these chains is similar to that of cholesterol. Therefore, environmentally induced *cis-trans* isomerization of the double bond should result in a stronger effect of carotenoids (or similar molecules) on the hydrocarbon chains in the bacterial membrane whenever it contains carotenoid-like molecules. The structure of the lipid matrix of the membrane would then become more rigid and hydrophobic and thus less permeable for polar molecules and ions. In this way, bacterial cell membrane integrity would be better preserved and the cell could better sustain stressful external conditions.

CONCLUSIONS

This MD simulation study confirmed numerous experimental results, particularly that the order and rotational diffusion of mono-*cis*-unsaturated, mono-*trans*-unsaturated, and saturated chains do not differ significantly from one another. This study also confirmed both experimental and computer simulation results that torsion angles of saturated C-C bonds next to the *cis* double bond are broadly distributed (in the range between 60 and 300°) and the *gauche* probability for the second next torsions to the *cis* double bond is higher than in a fully saturated chain.

This study provided the following new results: (1) Torsion angles of saturated C-C bonds next to the *trans* double bond continuously populated the whole range of angles between 0 and 360°. This makes the mono-*trans*-unsaturated chain more adaptive than the mono-*cis*-unsaturated chain and in many respects similar to a fully saturated chain. (2) The intrinsic effect of the *cis* double bond on β_4 and β_5 torsions angles is very similar to the extrinsic effect of cholesterol on these angles in a fully saturated chain. Both in the POPC and DMPC-cholesterol bilayers, the *gauche* probability of β_4 and β_5 is much higher and lower, respectively, than that in the pure DMPC bilayer. (3) The packing of the alkyl chains in a mono-*trans*-unsat-

urated bilayer is similar to that in a saturated bilayer, whereas the packing of the alkyl chains in a mono-*cis*-unsaturated bilayer is significantly looser. **FIG**

The authors thank W. K. Subczynski for helpful discussions. K.M and T.R. hold fellowship awards from the Polish Foundation for Science. This work was supported in part by grant 6P04A03121 from the Polish Committee for Scientific Research. All calculations were performed at the academic Computer Centre *Cyfronet* in Krakow, Poland, for which grant numbers KBN/SGI_ORIGIN_2000/004/2000 and KBN/SGI_ORIGIN_2000/062/1999 apply.

REFERENCES

- Small, D. M. 1998. Potpourri: effects of unsaturation on lipid structure; plasma cholesterol ester and lipid-transfer proteins; and cholesterol-sensing proteins and cellular cholesterol movement. *Curr. Opin. Struct. Biol.* **8**: 413–416.
- Dubertret, G., A. Mirshahi, M. Mirshahi, C. Gerard-Hirne, and A. Tremolieres. 1994. Evidence from *in vivo* manipulations of lipid composition in mutants that the Δ^3 -*trans*-hexadecenoic acid-containing phosphatidylglycerol is involved in the biogenesis of the light-harvesting chlorophyll *a/b*-protein complex of *Chlamydomonas reinhardtii*. *Eur. J. Biochem.* **226**: 473–482.
- Ohnishi, M., and G. A. Thompson, Jr. 1991. Biosynthesis of the unique *trans*- Δ^3 -hexadecenoic acid component of chloroplast phosphatidylglycerol: evidence concerning its site and mechanism of formation. *Arch. Biochem. Biophys.* **288**: 591–599.
- Gillan, F. T., R. B. Johns, T. V. Verheyen, J. K. Volkman, and H. J. Bavor. 1981. *Trans*-monounsaturated acids in a marine bacterial isolate. *Appl. Environ. Microbiol.* **41**: 849–856.
- Keweloh, H., and H. J. Heipieper. 1996. *Trans* unsaturated fatty acids in bacteria. *Lipids.* **31**: 129–137.
- Lamberto, M., and R. G. Ackman. 1994. Confirmation by gas chromatography/mass spectrometry of two unusual *trans*-3-monoethylenic fatty acids from Nova Scotian seaweeds *Palmaria palmata* and *Chondrus crispus*. *Lipids.* **29**: 441–444.
- Okuyama, H., N. Okajima, S. Sasaki, S. Higashi, and N. Murata. 1991. The *cis/trans* isomerization of the double bond of a fatty acid as a strategy for adapting to changes in ambient temperature in the psychrophilic bacterium, *Vibrio* sp. strain ABE-1. *Biochim. Biophys. Acta.* **1084**: 13–20.
- Kieft, T. L., D. B. Ringelberg, and D. C. White. 1994. Changes in ester-linked phospholipid fatty acid profiles of subsurface bacteria during starvation and desiccation in a porous medium. *Appl. Environ. Microbiol.* **60**: 3292–3299.
- Heipieper, H. J., R. Diefenbach, and H. Keweloh. 1992. Conversion of *cis* unsaturated fatty acids to *trans*, a possible mechanism for the protection of phenol-degrading *Pseudomonas putida* P8 from substrate toxicity. *Appl. Environ. Microbiol.* **58**: 1847–1852.
- Kaneko, F., J. Yano, and K. Sato. 1998. Diversity in the fatty-acid conformation and chain packing of *cis*-unsaturated lipids. *Curr. Opin. Struct. Biol.* **8**: 417–425.
- Di, L., and D. M. Small. 1995. Physical behavior of the hydrophobic core of membranes: properties of 1-stearoyl-2-linoleoyl-*sn*-glycerol. *Biochemistry.* **34**: 16672–16677.
- Davis, J. H. 1983. The description of membrane lipid conformation, order and dynamics by ^2H -NMR. *Biochim. Biophys. Acta.* **737**: 117–171.
- Stubbs, C., and A. D. Smith. 1984. The modification of mammalian membrane polyunsaturated fatty acid composition in relation to membrane fluidity and function. *Biochim. Biophys. Acta.* **779**: 89–137.
- Applegate, K. R., and J. A. Glomset. 1991. Effect of acyl chain unsaturation on the packing of model diacylglycerols: a computer modeling study. *J. Lipid Res.* **32**: 1645–1655.
- Huang, C-h. 2001. Mixed-chain phospholipids: structures and chain melting behavior. *Lipids.* **36**: 1077–1097.
- Koyanova, R., and M. Caffrey. 1998. Phases and phase transitions of the phosphatidylcholines. *Biochim. Biophys. Acta.* **1376**: 91–145.
- Wang, G., H-n. Lin, S. Li, and C-h Huang. 1995. Phosphatidylcholine with *sn*-1 saturated and *sn*-2 *cis*-monounsaturated acyl chains. *J. Biol. Chem.* **270**: 22738–22746.
- Seelig, J., and N. Waespe-Sarčević. 1978. Molecular order in *cis* and *trans* unsaturated phospholipid bilayers. *Biochemistry.* **17**: 3310–3315.
- Stubbs, C., T. Kouyama, K. Kinoshita, and A. Ikegami. 1981. Effect of double bonds on the dynamics properties of the hydrocarbon region of lecithin bilayers. *Biochemistry.* **20**: 4257–4262.
- Kusumi, A., W. K. Subczynski, M. Pasenkiewicz-Gierula, J. S. Hyde, and H. Merkle. 1986. Spin-label studies of phosphatidylcholine-cholesterol membranes: effects of alkyl chain length and unsaturation in the fluid phase. *Biochim. Biophys. Acta.* **854**: 307–317.
- Subczynski, W. K., and A. Wisniewska. 1996. Three-dimensional structure of the lipid bilayer membranes: an EPR spin label study. *Cell. Mol. Biol. Lett.* **1**: 377–389.
- Yin, J-J., and W. K. Subczynski. 1996. Effects of lutein and cholesterol on alkyl chain bending in lipid bilayers: a pulse electron spin resonance spin labeling study. *Biophys. J.* **71**: 832–839.
- Yin, J-J., J. B. Feix, and J. S. Hyde. 1990. Mapping of collision frequencies for stearic acid spin labels by saturation-recovery electron paramagnetic resonance. *Biophys. J.* **58**: 713–720.
- Subczynski, W. K., W. E. Antholine, J. S. Hyde, and A. Kusumi. 1990. Microimmiscibility and three-dimensional dynamic structures of phosphatidylcholine-cholesterol membranes: translational diffusion of a copper complex in the membrane. *Biochemistry.* **29**: 7936–7945.
- Subczynski, W. K., J. S. Hyde, and A. Kusumi. 1991. Effect of alkyl chain unsaturation and cholesterol intercalation on oxygen transport in membranes: a pulse ESR spin labeling study. *Biochemistry.* **30**: 8578–8590.
- Subczynski, W. K., A. Wisniewska, J-J. Yin, J. S. Hyde, and A. Kusumi. 1994. Hydrophobic barriers of lipid bilayer membranes formed by reduction of water penetration by alkyl chain unsaturation and cholesterol. *Biochemistry.* **33**: 7670–7681.
- Pearce, L. L., and S. C. Harvey. 1993. Langevin dynamics studies of unsaturated phospholipids in a membrane environment. *Biophys. J.* **65**: 1084–1092.
- Heller, H., M. Scheafer, and K. Schulten. 1993. Molecular dynamics simulation of a bilayer of 200 lipids in the gel and in the liquid-crystal phases. *J. Phys. Chem.* **97**: 8343–8360.
- Huang, P., J. J. Perez, and G. H. Loew. 1994. Molecular dynamics simulations of phospholipid bilayers. *J. Biomol. Struct. Dyn.* **11**: 927–956.
- Bolterauer, C., and H. Heller. 1996. Calculation of IR dichroic values and order parameters from molecular dynamics simulation and their application to structure determination of lipid bilayers. *Eur. Biophys. J.* **24**: 322–334.
- Feller, S. E., D. Yin, R. W. Pastor, and A. D. MacKerell. 1997. Molecular dynamics simulation of unsaturated lipid bilayers at low hydration: parameterization and comparison with diffraction studies. *Biophys. J.* **73**: 2269–2279.
- Feller, S. E., K. Gawrisch, and A. D. MacKerell, Jr. 2002. Polyunsaturated fatty acids in lipid bilayers: intrinsic and environmental contributions to their unique physical properties. *J. Am. Chem. Soc.* **124**: 318–326.
- Hyvönen, M. T., T. T. Rantala, and M. Ala-Korpela. 1997. Structure and dynamic properties of diunsaturated 1-palmitoyl-2-linoleoyl-*sn*-glycero-3-phosphatidylcholine lipid bilayer from molecular dynamics simulation. *Biophys. J.* **73**: 2907–2923.
- Armen, R. S., O. D. Uitto, and S. E. Feller. 1998. Phospholipid component volumes: determination and application to bilayer structure calculation. *Biophys. J.* **75**: 734–744.
- Chiu, S. W., E. Jacobsson, S. Subramaniam, and H. L. Scott. 1999. Combined Monte Carlo and molecular dynamics simulation of fully hydrated dioleoyl and palmitoyl-oleyl phosphatidylcholine lipid bilayers. *Biophys. J.* **77**: 2462–2469.
- Murzyn, K., T. Róg, G. Jezierski, Y. Takaoka, and M. Pasenkiewicz-Gierula. 2001. Effects of phospholipid unsaturation on the membrane-water interface: a molecular simulation study. *Biophys. J.* **81**: 170–183.
- Mashl, R. J., H. L. Scott, S. Subramaniam, and E. Jacobsson. 2001. Molecular simulation of dioleoylphosphatidylcholine lipid bilayers at differing levels of hydration. *Biophys. J.* **82**: 3005–3015.
- Huber, T., K. Rajamoorthi, V. F. Kurze, K. Beyer, and M. F. Brown. 2002. Structure of docosahexaenoic acid-containing phospholipid bilayers as studied by ^2H NMR and molecular dynamics simulations. *J. Am. Chem. Soc.* **124**: 298–309.

39. Di, L., and D. M. Small. 1993. Physical behavior of the mixed chain diacylglycerol, 1-stearoyl-2-oleoyl-*sn*-glycerol: difficulties in chain packing produce marked polymorphism. *J. Lipid Res.* **34**: 1611–1623.
40. Applegate, K. R., and J. A. Glomset. 1991. Effect of acyl chain unsaturation on the conformation of model diacylglycerols: a computer modeling study. *J. Lipid Res.* **32**: 1635–1644.
41. Li, S., H.-n. Lin, Z.-q. Wang, and C. Huang. 1994. Identification and characterization of kink motifs in 1-palmitoyl-2-linoleoyl-phosphatidylcholines: a molecular mechanics study. *Biophys. J.* **66**: 2005–2018.
42. Murzyn, K., T. Róg, and M. Pasenkiewicz-Gierula. 1999. Comparison of the conformation and the dynamics of saturated and mono-unsaturated hydrocarbon chains of phosphatidylcholines. *Curr. Top. Biophys.* **23**: 87–94.
43. Holte, L. L., S. A. Peter, T. M. Sinnwell, and K. Gawrisch. 1995. ^2H nuclear magnetic resonance order parameter profiles suggest a change of molecular shape for phosphatidylcholines containing a polyunsaturated acyl chain. *Biophys. J.* **68**: 2396–2403.
44. Pasenkiewicz-Gierula, M., Y. Takaoka, H. Miyagawa, K. Kitamura, and A. Kusumi. 1997. Hydrogen bonding of water to phosphatidylcholine in the membrane as studied by a molecular dynamics simulation: location, geometry and lipid-lipid bridging via hydrogen bonded water. *J. Chem. Phys.* **101**: 3677–3691.
45. Pasenkiewicz-Gierula, M., Y. Takaoka, H. Miyagawa, K. Kitamura, and A. Kusumi. 1999. Charge pairing of headgroups in phosphatidylcholine membranes: a molecular dynamics simulation study. *Biophys. J.* **76**: 1228–1240.
46. Jorgensen, W. L., and J. Tirado-Rives. 1988. The OPLS potential functions for proteins. Energy minimizations for crystals of cyclic peptides and crambin. *J. Am. Chem. Soc.* **110**: 1657–1666.
47. Jorgensen, W. L., J. Chandrasekhar, J. D. Madura, R. W. Impey, and M. L. Klein. 1983. Comparison of simple potential functions for simulating liquid water. *J. Chem. Phys.* **79**: 926–935.
48. Pearlman, D. A., D. A. Case, J. C. Caldwell, G. L. Seibel, U. C. Singh, P. K. Weiner, and P. A. Kollman. 1991. AMBER 4.0. San Francisco, University of California.
49. Case, D. A., D. A. Pearlman, J. W. Caldwell, T. E. Cheatham III, W. S. Ross, C. Simmerling, T. A. Darden, K. M. Merz, R. V. Stanton, A. L. Cheng, J. J. Vincent, M. Crowley, D. M. Ferguson, R. J. Radmer, G. L. Seibel, U. C. Singh, P. K. Weiner, and P. A. Kollman. 1997. AMBER 5.0. San Francisco, University of California.
50. Ryckaert, J. P., G. Cicotti, and H. J. C. Berendsen. 1977. Numerical integration of the Cartesian equations of motion of a system with constraints: molecular dynamics of n-alkanes. *J. Comp. Phys.* **22**: 327–341.
51. Egberts, E., S.J. Marrink, and H. J. C. Berendsen. 1994. Molecular dynamics simulation of a phospholipid membrane. *Eur. Biophys. J.* **22**: 432–436.
52. Berendsen, H. J. C., J. P. M. Postma, W. F. van Gunsteren, A. Dinola, and J. R. Haak. 1984. Molecular dynamics with coupling to an external bath. *J. Chem. Phys.* **81**: 3684–3690.
53. Róg, T., and M. Pasenkiewicz-Gierula. 2001. cholesterol effects on the phosphatidylcholine bilayer nonpolar region: a molecular simulation study. *Biophys. J.* **81**: 2190–2202.
54. Smaby, J. M., M. M. Momsen, H. L. Brockman, and R. E. Brown. 1997. Phosphatidylcholine acyl unsaturation modulates the decrease in the interfacial elasticity induced by cholesterol. *Biophys. J.* **73**: 1492–1505.
55. Hyslop, P. A., B. Morel, and R. D. Sauerheber. 1990. Organization and interaction of cholesterol and phosphatidylcholine in model bilayer membrane. *Biochemistry.* **29**: 1025–1038.
56. Nagle, J. F., and S. Tristram-Nagle. 2000. Structure of lipid bilayer. *Biochim. Biophys. Acta.* **1469**: 159–195.
57. Ueno, S., T. Suetake, J. Yano, M. Suzuki, and K. Sato. 1994. Structure and polymorphic transformations in elaidic acid (*trans*- ω 9-octadecenoic acid). *Chem. Phys. Lipids.* **72**: 27–34.
58. Pasenkiewicz-Gierula, M., W. K. Subczynski, and A. Kusumi. 1991. Influence of phospholipid unsaturation on the cholesterol distribution in membranes. *Biochimie.* **73**: 1311–1316.
59. Yokoyama, A., G. Sandmann, T. Hoshino, K. Adachi, M. Sakai, and Y. Shizuri. 1995. Thermozeaxanthins, new carotenoid-glycoside ester from thermophilic eubacterium *Thermus thermophilus*. *Tetrahedron Lett.* **36**: 4901–4904.
60. Oren, A., and F. Rodriguez-Valera. 2001. The contribution of halophilic bacteria to the red coloration of saltern crystallizer ponds. *FEMS Microbiol. Ecol.* **36**: 123–130.
61. Subczynski, W. K., E. Markowska, and J. Siewiewsiuk. 1993. Spin-label studies on phosphatidylcholine-polar carotenoid membrane: effects of alkyl-chain length and unsaturation. *Biochim. Biophys. Acta.* **1150**: 173–181.
62. Wisniewska, A., and W. K. Subczynski. 1997. Effects of polar carotenoids on the shape of the hydrophobic barrier of phospholipid bilayers. *Biochim. Biophys. Acta.* **1368**: 235–246.